Error Dynamics and Perfect Model Following with Application to Flight Control

Mark R. Anderson*
Systems Control Technology, Inc., Lexington Park, Maryland 20653
and
David K. Schmidt†
Arizona State University, Tempe, Arizona 85287

The role of the system error dynamics in model-following control systems is presented in a unified theoretical framework. The approach clearly exposes the requirements for perfect model-following control laws to exist. The error dynamics selected are shown to determine if implicit or explicit following results, and the effects of these error dynamics and plant and model dynamics on the closed-loop stability, performance, and control system architecture are exposed. The importance of model and plant transmission zeros is also revealed. A new linear quadratic formulation is offered that can yield perfect model-following controllers, but guarantees internal system stability, unlike algebraic solutions for the control law. Further, the case of finite actuation bandwidth may be treated with the linear quadratic approach. The error dynamics are also shown to be key in this linear quadratic model-following formulation. The paper concludes with an example involving an unstable forward-swept-wing elastic aircraft, which demonstrates that high-fidelity model-following control laws can be synthesized for statically unstable aircraft with nonminimum phase transmission zeros.

Introduction

MODEL-FOLLOWING control synthesis techniques can be used, for example, to incorporate flight vehicle handling qualities specifications directly into the design process. In this paper, the relationships that define the system error, error dynamics, and resulting loop properties of model-following controllers are developed. These relationships are then used to reveal the implications of the model chosen and the unaugmented vehicle dynamics on the resulting characteristics of the feedback system.

The importance of the system error in model-following synthesis was noted, for example, in the pioneering work of Rynaski et al.[1] Several combinations of system error and error rate were weighted in linear quadratic regulator (LQR) cost functions in order to obtain model-following control laws. It was shown that error rate must be used to yield perfect following. Detailed analysis of these results led Tyler[2] to the conclusion that the feedback gains of the linear, quadratic (explicit) model-following problem were also independent of the model dynamics. This result led to the conclusion that the feedback gains can be used to vary the system error dynamics. Other researchers then developed model-following algorithms that directly defined the system error dynamics in a variety of ways. Most notable are the methods developed by Chan,[3] Davison,[4] Kawahata,[5] and Buethe and Lebacqz.[6]

The focus of this paper is on developing a unifying framework such that the effects of the plant and model dynamics and the chosen model-following system error dynamics on the closed-loop stability, performance, and the resulting control system structure are readily apparent. Furthermore, in almost all of the past work, the model and plant are assumed to be of equal dimension, with the error vector defined as the difference between the two state vectors. In this work, the error vector is defined as the difference between the response vectors, which may be of lower dimension than the state, and allows for plant and model to be of different dimension. Finally, two examples are included to illustrate the results.

Perfect Model Following

Consider the linear, time-invariant (LTI) representation of the vehicle dynamics to be

$$\dot{x} = Ax + Bu, \qquad \dim(x) = n, \qquad \dim(u) = m \le n$$

$$y = Cx, \qquad \dim(y) = p \le n \tag{1}$$

and an LTI representation of the desired model dynamics to be

$$\dot{x}_m = A_m x_m + B_m \delta, \qquad \dim(x_m) = q \ge p$$

$$y_m = C_m x_m, \qquad \dim(y_m) = p \tag{2}$$

We will assume throughout, unless otherwise noted, that the first Markov parameter of the vehicle (1) has maximum rank [i.e., $\text{rank}(CB) = \min(p,m)$] and that p is not less than m. (In cases for which p is less than m, some control inputs need not be included or may be blended together such that the assertion is true.) The system error is defined as the difference between the vehicle and model responses, with the model excited by some external input δ (such as a pilot stick input) or

$$e = y - y_m, \qquad \dim(e) = p$$

Also, the system error rate is

$$\dot{e} = \dot{y} - \dot{y}_m = C(Ax + Bu) - C_m(A_m x_m + B_m \delta)$$

The control law required to achieve stable, homogeneous error dynamics is the control u, found such that

$$\dot{e} + Ee = 0 \tag{3}$$

Presented as Paper 87-2311 at the AIAA Guidance, Navigation, and Control Conference, Monterey, CA, Aug. 17–19, 1987; received May 31, 1988; revision received July 23, 1990; accepted for publication Aug. 9, 1990.

*Engineer. Member AIAA.

†Professor of Engineering; Acting Director, Aerospace Research Center, College of Engineering and Applied Science. Associate Fellow AIAA.

where the error dynamics are defined by selection of the matrix E. Thus,

$$CAx + CBu - C_m A_m x_m - C_m B_m \delta + E(Cx - C_m x_m) = 0 \quad (4)$$

or

$$u = -(CB)^{+}[(CA + EC)x - (C_m A_m + EC_m)x_m - C_m B_m \delta] \quad (5)$$

where $(CB)^{+}$ is the generalized inverse of CB.

Conditions for perfect model following have been developed by both Erzberger[7] and Chan.[3] Somewhat more general conditions for the case considered in this work may be obtained directly by using the control law (5) in the error equation (4) to yield,

$$(CA + EC)x - (C_m A_m + EC_m)x_m - C_m B_m \delta - (CB)(CB)^{+}$$
$$\times [(CA + EC)x - (C_m A_m + EC_m)x_m - C_m B_m \delta] = 0$$

This equation will obviously hold if the following conditions are met:

$$[I - CB(CB)^{+}]\,(CA + EC) = 0 \quad (6)$$

$$[I - CB(CB)^{+}]\,(C_m A_m + EC_m) = 0 \quad (7)$$

$$[I - CB(CB)^{+}]\,C_m B_m = 0 \quad (8)$$

One can now write the model-following control law (5) as,

$$u = -Kx - K_m x_m - K_\delta \delta \quad (9)$$

with appropriate definitions for K, K_m, K_δ.

Note that the conditions (6–8) are always satisfied when CB is square and nonsingular, but may also be satisfied in other, more general cases. Under these more general conditions, Eqs. (6–8) place restrictions on the model, plant, and error dynamics.

The closed-loop system is

$$\begin{bmatrix} \dot{x} \\ \dot{x}_m \end{bmatrix} = \begin{bmatrix} A - BK & -BK_m \\ 0 & A_m \end{bmatrix} \begin{bmatrix} x \\ x_m \end{bmatrix} + \begin{bmatrix} -BK_\delta \\ B_m \end{bmatrix} \delta \quad (10a)$$

$$y = [C \quad 0] \begin{bmatrix} x \\ x_m \end{bmatrix} \quad (10b)$$

and the closed-loop system eigenvalues are those of the augmented vehicle, $A - BK$, and of the model, A_m. Note in Fig. 1 that the model dynamics appear in a prefilter and the gains in K augment the vehicle dynamics. Since, by inspection of Eqs. (6–9), and as reported by Tyler,[2] the feedback gains K do not depend on the model dynamics, some design freedom exists in the feedback loop dynamics.

The dynamics of the feedback loop can be clearly understood by considering a coordinate transformation T where

$$\begin{bmatrix} y \\ w \end{bmatrix} = \begin{bmatrix} C \\ M \end{bmatrix} x = Tx \quad (11)$$

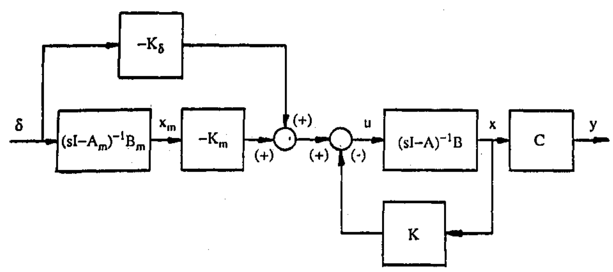

Fig. 1 Explicit model-following control law.

and M is chosen such that T^{-1} exists, $(TT^{-1} = I_n$, $T^{-1}T = I_n)$. Defining $T^{-1} = [C_{-1} M_{-1}]$, the following properties result

$$CC_{-1} = I_p \quad (12a)$$

$$MM_{-1} = I_{n-p} \quad (12b)$$

$$CM_{-1} = 0 \quad (12c)$$

$$MC_{-1} = 0 \quad (12d)$$

$$C_{-1}C + M_{-1}M = I_n \quad (12e)$$

Now, by applying transformation (11) to the augmented plant dynamics

$$\dot{x} = (A - BK)x$$

we have

$$\begin{bmatrix} \dot{y} \\ \dot{w} \end{bmatrix} = \begin{bmatrix} C(A - BK)C_{-1} & C(A - BK)M_{-1} \\ M(A - BK)C_{-1} & M(A - BK)M_{-1} \end{bmatrix} \begin{bmatrix} y \\ w \end{bmatrix}$$

Assuming perfect model following, from Eq. (6) and the definition of K we have

$$C(A - BK) + EC = 0 \quad (13)$$

so that

$$C(A - BK)M_{-1} + ECM_{-1} = 0$$

But, since $CM_{-1} = 0$, from Eqs. (12),

$$C(A - BK)M_{-1} = 0$$

Therefore, with perfect model following, the response y is decoupled from the response w. Also, because of this decoupling, the closed-loop poles of the augmented plant $A - BK$ are the eigenvalues of $C(A - BK)C_{-1}$ and $M(A - BK)M_{-1}$.

From Eq. (13),

$$C(A - BK)C_{-1} + ECC_{-1} = 0$$

or since $CC_{-1} = I$ by Eqs. (12), the error dynamics are

$$C(A - BK)C_{-1} = -E$$

Also, by the definition of K,

$$M(A - BK)M_{-1} = M[I - B(CB)^{+}C]AM_{-1}$$

Therefore, the freedom that exists in selecting the augmented plant dynamics is limited to the selection of p eigenvalues of the error dynamics arbitrarily. The remaining $(n - p)$ eigenvalues will be the eigenvalues of $M[I - B(CB)^{+}C]AM_{-1}$. Hence, selection of the error dynamics, the control vector u, and the following responses y completely specifies the augmented plant $(A - BK)$ poles.

Further, it has been shown by Morse[8] that when CB is square, the poles of $M[I - B(CB)^{+}C]AM_{-1}$ are also the finite transmission zeros of the open-loop plant $C(sI - A)^{-1}B$. Consequently, as noted by Kudva and Gourishankar,[9] the perfect model-following control law in Eq. (5) will place closed-loop poles at the transmission zeros of the open-loop plant, even if it results in an unstable system.

The effect of the error system and chosen model on the transmission zeros of the augmented vehicle is also of interest. Not only are certain pole locations desired, but certain zeros as well. Bringing EC to the right side of Eq. (13) and adding sC

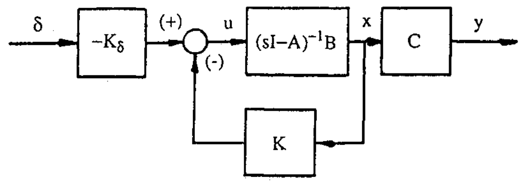

Fig. 2 Implicit model following control law.

to both sides yields

$$C[sI-(A-BK)] = [sI+E]C$$

or

$$[sI-(-E)]^{-1}C = C[sI-(A-BK)]^{-1}$$

Postmultiplying by BK_δ and noting [from Eqs. (5), (8), and (9)] that $C_mB_m = -CBK_\delta$, the preceding equation becomes

$$-[sI-(-E)]^{-1}C_mB_m = C[sI-(A-BK)]^{-1}BK_\delta$$

Assuming these systems are square, taking determinants of both sides of this equation defines the transmission zeros of the augmented vehicle on the right, or

$$|[sI-(-E)]^{-1}C_mB_m| = |C[sI-(A-BK)]^{-1}BK_\delta| = 0 \tag{14}$$

The right side of this equation defines the transmission zeros of the closed-loop and open-loop vehicle dynamics since they remain invariant under state feedback and nonsingular input transformations,[10] with the exception that these zeros are for stick input δ, rather than control input u. Equation (14) also relates these zeros to the transmission zeros of a system defined in terms of model response and input matrices and the error dynamics.

Looking further in the frequency domain, the loop transfer matrix for the feedback control law of Eq. (5) is

$$KG(s) = (CB)^+(EC+CA)(sI-A)^{-1}B$$

or after some manipulation,

$$KG(s) = (CB)^+[(sI+E)C(sI-A)^{-1}B - CB]$$

This relation reveals the relationship between the chosen error dynamics E and the loop transfer matrix KG, or the loop shape.

Implicit Model Following

Of primary concern, then, is how to choose the error dynamics. As a special case, consider the control law (9) once again. If through some choice of error dynamics $K_m = 0$, implicit model following results as the control law no longer is an explicit function of the model dynamics. This results in the simpler closed-loop system shown in Fig. 2.

For $K_m = 0$, we require, from Eq. (5),

$$C_mA_m + EC_m = 0$$

or

$$E = -C_mA_mC_{m-1} \tag{15}$$

where, similar to Eqs. (11) and (12), $T_m^{-1} = [C_{m-1}M_{m-1}]$ and

$$\begin{bmatrix} y_m \\ w_m \end{bmatrix} = \begin{bmatrix} C_m \\ M_m \end{bmatrix} x_m = T_m x_m$$

Note that, to satisfy Eq. (15), C_m is not restricted to be square and invertible, though such a case is obviously allowed. Also note that selecting E as in Eq. (15) does not guarantee that the equation before Eq. (15) is satisfied, as it must be for perfect following. This will, however, be satisfied when either C_m is invertible or if $C_mA_mM_{m-1} = 0$.

In transformed coordinates, now, the model dynamics are

$$\begin{bmatrix} \dot{y}_m \\ \dot{w}_m \end{bmatrix} = \begin{bmatrix} C_mA_mC_{m-1} & C_mA_mM_{m-1} \\ M_mA_mC_{m-1} & M_mA_mM_{m-1} \end{bmatrix} \begin{bmatrix} y_m \\ w_m \end{bmatrix} + \begin{bmatrix} C_mB_m \\ M_mB_m \end{bmatrix} \delta \tag{16}$$

Therefore, from Eq. (16), one can see that a subset of the model dynamics must be chosen as the error dynamics, or $E = -C_mA_mC_{m-1}$, in order to obtain an implicit model-following structure.

For perfect model following, we have, from Eq. (7),

$$[I - CB(CB)^+](C_mA_m + EC_m) = 0$$

Postmultiplying by C_{m-1}, and noting that $C_mC_{m-1} = I$, results in

$$[I - CB(CB)^+](C_mA_mC_{m-1} + E) = 0$$

but this is satisfied by Eq. (15). Postmultiplying on the right by M_{-1} and noting that $C_mM_{m-1} = 0$, we have the second condition for perfect implicit model following, or

$$[I - CB(CB)^+]C_mA_mM_{m-1} = 0$$

Therefore, if $[I - CB(CB)^+] \neq 0$, the preceding equation is satisfied if $C_mA_mM_{m-1} = 0$. In this case, responses y_m are decoupled from the other model responses w_m, and, in fact, only the lower-order model governing y_m need be used.

The model transmission zeros are also constrained for perfect, implicit model following. The constraint can be found from Eq. (14) and by noting that $E = -C_mA_mC_{m-1}$. Now, Eq. (14) becomes

$$|[sI - C_mA_mC_{m-1}]^{-1}C_mB_m| = |C[sI-(A-BK)]^{-1}BK_\delta| = 0$$

If $C_mA_mM_{m-1} = 0$ or if C_m is the identity, the left side of this equation defines the transmission zeros of the subsystem of the model dynamics (16) that are being followed.

Because the feedback gains used in implicit model following are chosen to make the closed-loop vehicle identical to the model, i.e, $A - BK \approx A_m$ and $-BK_\delta \approx B_m$, what results is a finely tuned feedback control augmenter that nominally does not increase the dynamic order of the response to pilot input. When the error dynamics are chosen different from the model dynamics, the more complex system in Fig. 1 results.

Integral Control

If integral action is desired, a simple extension of the preceding formulation leads to the desired result. Asseo[11] used a complicated weighting structure to develop a type − 1, perfect model-following system based on LQR theory. He also showed that by using his weighting conditions the resulting error dynamics would be

$$\dot{e} + E_1e + E_2z = 0 \tag{17}$$

where

$$z = \int_0^t e(\tau)\,d\tau$$

Similar to the development shown in Eqs. (3-9), Eq. (17) can be used directly to obtain the direct state-space control law,

$$u = -(CB)^+[(CA + E_1C)x - (C_mA_m + E_1C_m)x_m - C_mB_m\delta + E_2z]$$

The perfect model-following conditions required for this control law are

$$[I - CB(CB)^+](CA + E_1C) = 0$$

$$[I - CB(CB)^+](C_mA_m + E_1C_m) = 0$$

$$[I - CB(CB)^+]C_mB_m = 0$$

$$[I - CB(CB)^+]E_2 = 0$$

Examination of the loop transfer for this control law would reveal that integral action is present.

Example 1

Consider the second-order short-period approximation for an aircraft's pitch dynamics

$$\frac{q}{\delta_e} = \frac{M_{\delta e}(s + 1/\tau_{\theta_2})}{(s^2 + 2\zeta_{sp}\omega_{sp}s + \omega_{sp}^2)}$$

where q is the perturbed pitch rate and δ_e is the elevator deflection input. Also, let

$$1/\tau_{\theta_2} = -Z_\alpha/U_1$$

$$\zeta_{sp} = \frac{-(M_q + Z_\alpha/U_1)}{2\omega_{sp}}$$

$$\omega_{sp}^2 = Z_\alpha M_q/U_1 - M_\alpha$$

where $M_{\delta e}$, Z_α, M_q, and M_α are the traditional longitudinal stability derivatives[12] and U_1 is the aircraft trim velocity. Table 1 includes the numerical values for the example flight condition.

At the design condition, the short-period damping is $\zeta_{sp} = 0.14$. It is desired to increase this value to $\zeta_m = 0.6$. Let the state-space representation of the vehicle dynamics be

$$\begin{bmatrix} \dot{x}_1 \\ \dot{x}_2 \end{bmatrix} = \begin{bmatrix} 0 & 1 \\ -\omega_{sp}^2 & -2\zeta_{sp}\omega_{sp} \end{bmatrix} \begin{bmatrix} x_1 \\ x_2 \end{bmatrix} + \begin{bmatrix} 0 \\ M_{\delta e} \end{bmatrix} \delta_e$$

$$q = 1/\tau_{\theta_2} x_1 + x_2$$

and let the model dynamics have the same form.

Case 1

An implicit model-following control law is obtained by choosing the error vector as $e = x - x_m$. It is necessary to have $\dim(e) = 2$ in order to place both vehicle poles exactly. Therefore, with $C = C_m = I$, choosing the error dynamics as $E = -A_m$ yields $K_m = 0$ and implicit model-following results. One can readily verify that the perfect model-following conditions (6–8) are met. The feedback gains, in this case, can be found from the definition of K to be

$$K = 1/M_{\delta e}[(\omega_m^2 - \omega_{sp}^2), 2(\zeta_m\omega_m - \zeta_{sp}\omega_{sp})]$$

By choosing

$$\zeta_m = \frac{K_q M_{\delta e} + 2\zeta_{sp}\omega_{sp}}{2\omega_m}$$

$$\omega_m^2 = \frac{K_q M_{\delta e}}{\tau_{\theta_2}} + \omega_{sp}^2$$

the following feedback control law results:

$$u = -K_q[1/\tau_{\theta_2} \;\; 1]\begin{bmatrix} x_1 \\ x_2 \end{bmatrix} + \delta_{ec} \tag{18}$$

or $u = -K_q q + \delta_{ec}$, which is simply the feedback control law for a pitch damper.

Table 1 Example 1—design condition

Transfer function parameter	Value
$M_{\delta e}$, 1/s²	0.26
M_q, 1/s	0.21
M_α, 1/s²	− 4.69
Z_α, ft/s²	− 166.0
U_1, ft/s	205.0
$1/\tau_{\theta 2}$, 1/s	0.81
ω_{sp}, rad/s	2.13
ζ_{sp}	0.14

Case 2

For simplicity of implementation, assume the pitch-rate feedback control law (18) is to be retained, but with K_q increased to 40 from 9.5 rads/rad. The augmented vehicle dynamics become

$$A - BK = \begin{bmatrix} 0 & 1 \\ -12.96 & -11.00 \end{bmatrix}$$

with poles (equal to the error-dynamic poles) now at -1.34 and -9.66 rad/s. Explicit model following is now required, and the model feed-forward gains $K_m = -(CB)^+(C_mA_m + EC_m)$ are found by noting that, when $C = I$, the augmented vehicle dynamics and the error dynamics are the same. Perfect model following is still obtained, but the loop gain has increased, moving the gain-crossover frequency of the feedback loop out to 10 rad/s, compared to about 4 rad/s for case 1.

Case 3

Now let the two error poles be at -5.0 rad/s, so the desired error dynamics become

$$E = -\begin{bmatrix} 0 & 1 \\ -25.0 & -10.0 \end{bmatrix}$$

The feed-forward and feedback gains may be found from Eq. (5). In particular, the feedback gains are now

$$K = [78.70 \quad 36.17]$$

Because these error poles were chosen without regard to the structure of the feedback control law, both vehicle states must be fed back in this case. A simple output observer can be constructed by noting that the first state x_1 is approximately angle of attack α. The state transformation,

$$\begin{bmatrix} q \\ \alpha \end{bmatrix} = \begin{bmatrix} 1/\tau_{\theta_2} & 1 \\ 1 & 0 \end{bmatrix} \begin{bmatrix} x_1 \\ x_2 \end{bmatrix}$$

can then be used to find equivalent feedback gains on the physical states pitch rate and angle of attack. Under the short-period approximation,

$$\frac{\alpha}{q} = \frac{1}{s + 1/\tau_{\theta_2}}$$

and an estimate of angle of attack can be derived from pitch rate, resulting in a dynamic feedback compensator requiring only pitch rate for implementation of the control law. This estimator is also used in the next case. Again, perfect model following is achieved, and the gain-crossover frequency remains at 10 rad/s.

Case 4

Integral action can be added to the model-following control law, if desired, by selecting E_1 and E_2 in Eq. (17) to be

$$E_1 = \begin{bmatrix} 0 & -1 \\ 75 & 15 \end{bmatrix} \qquad E_2 = \begin{bmatrix} 0 & 0 \\ 125 & 0 \end{bmatrix}$$

Table 2 Control law transfer functions

Case	$P(s)$, rad/rad	$K(s)$, rad/rad
1	1.0	9.5
2	$\frac{(s+1.3)(s+9.6)}{[s^2+2(0.6)(2.56)s+(2.56)^2]}$	40.0
3	$\frac{(s+5.0)^2}{[s^2+2(0.6)(2.56)s+(2.56)^2]}$	$\frac{36.2(s+2.2)}{(s+0.81)}$
4	$\frac{(s+5.0)^3}{[s^2+2(0.6)(2.56)s+(2.56)^2]}$	$\frac{55.5[s^2+2(0.83)(2.95)s+(2.95)^2]}{s(s+0.81)}$

The three poles of the error dynamics will be at -5.0 rad/s, and perfect model following results. However, inspection of the loop transfer would reveal the presence of integral action in the loop.

The four control laws developed earlier are summarized in Table 2 for comparison. The block diagram in Fig. 3 shows the location of the prefilter $P(s)$ and feedback compensator $K(s)$ common to all cases. All of the control laws result in perfect model following at the design condition. However, in each successive case, the control law required has increased in complexity.

Linear Quadratic Formulation for Practical Model Following

As noted earlier, the perfect model-following controller can yield an unstable system if the plant has right-half-plane transmission zeros. Also, perfect model following is not always achievable with real systems. Consequently, another synthesis technique is sought that may yield more practical results. A new LQR formulation of the model-following problem is offered. The cost function is chosen to reflect the desire to arbitrarily choose the error dynamics. Or by divine inspiration, let

$$J_1 = \int_0^\infty [(\dot{e}+Ee)^TQ(\dot{e}+Ee)+u^TRu]\,dt \tag{19}$$

The constraint equations are

$$\begin{bmatrix}\dot{x}\\ \dot{x}_m\\ \dot{\delta}\end{bmatrix} = \begin{bmatrix}A & 0 & 0\\ 0 & A_m & B_m\\ 0 & 0 & A_P\end{bmatrix}\begin{bmatrix}x\\ x_m\\ \delta\end{bmatrix} + \begin{bmatrix}B\\ 0\\ 0\end{bmatrix}u$$

$$\begin{bmatrix}e\\ \dot{e}\end{bmatrix} = \begin{bmatrix}C & -C_m & 0\\ CA & -C_mA_m & -C_mB_m\end{bmatrix}\begin{bmatrix}x\\ x_m\\ \delta\end{bmatrix} + \begin{bmatrix}0\\ CB\end{bmatrix}u$$

where A_p represents a fictitious stick shaping filter that will not appear in the final control law. Note that this linear quadratic (LQ) formulation differs from that offered by Rynaski et al.[1] and Buethe and Lebacqz,[6] but will still yield a perfect model-following control law when the appropriate existence conditions are met. This can be shown by manipulation of the Riccati equation for this formulation and by applying the perfect model-following conditions (6–8). Also, through selection of the error dynamics, as discussed earlier, implicit as well as explicit model-following control laws may be synthesized.

This LQ problem will have a solution as long as $R+(CB)^TQCB$ is positive definite. If $p \geq m$ and $R=0$, a finite-gain solution will exist only if CB is full rank and Q is positive definite. It is also well known (see Ref. 13) that, when CB is square, the poles of the LQR will approach the (stable) finite transmission zeros of the open-loop system as R approaches the null matrix. The transmission zeros in this case

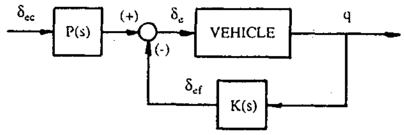

Fig. 3 Example 1—control law.

(with $Q=I$) are the roots of

$$\det[sI+E]\,\det[C(sI-A)^{-1}B]=0 \tag{20}$$

For systems with nonminimum phase transmission zeros, the regulator poles will approach their stable mirror image. Therefore, when CB is square and full rank, the cost function of Eq. (19) can deliver perfect model following, but with a guarantee of internal stability. Note, however, that although stability is theoretically guaranteed using this quadratic formulation, there are no guaranteed stability robustness margins[12] since $R+(CB)^TQCB$ does not, in general, have the required diagonal form.

When integral action is desired, Eq. (17) can be used to obtain a modified cost function, or

$$J_2 = \int_0^\infty [(\dot{e}+E_1e+E_2z)^TQ(\dot{e}+E_1e+E_2z)+u^TRu]\,dt \tag{21}$$

subject to the constraint equations

$$\begin{bmatrix}\dot{x}\\ \dot{x}_m\\ \dot{\delta}\\ \dot{z}\end{bmatrix} = \begin{bmatrix}A & 0 & 0 & 0\\ 0 & A_m & B_m & 0\\ 0 & 0 & A_P & 0\\ C & -C_m & 0 & 0\end{bmatrix}\begin{bmatrix}x\\ x_m\\ \delta\\ z\end{bmatrix} + \begin{bmatrix}B\\ 0\\ 0\\ 0\end{bmatrix}u$$

$$\dot{e}+E_1e+E_2z$$

$$= [(CA+E_1C) \quad -(C_mA_m+E_1C_m) \quad -C_mB_m \quad E_2]$$

$$\times \begin{bmatrix}x\\ x_m\\ \delta\\ z\end{bmatrix} + [CB]u$$

This formulation leads to the same type $-$ 1 systems reported by Asseo[11] with stable internal dynamics.

Actuators

In reality, the designer is always faced with finite bandwidth actuators. With actuation, the system dynamics are

$$\begin{bmatrix}\dot{x}_v\\ \dot{x}_a\end{bmatrix} = \begin{bmatrix}A_v & B_vC_a\\ 0 & A_a\end{bmatrix}\begin{bmatrix}x_v\\ x_a\end{bmatrix} + \begin{bmatrix}0\\ B_a\end{bmatrix}u$$

$$y = [C_v \quad 0]\begin{bmatrix}x_v\\ x_a\end{bmatrix} \tag{22}$$

where

$$\dot{x}_a = A_ax_a + B_au$$

is the linear model for the actuators, and the matrix triple (A_v, B_v, C_v) represents the airframe dynamics. By observation, one can see that $CB=0$ for this system, and so perfect model following can never be achieved, and the algebraic determination of the control law is not appropriate. However, with a slight variation in the LQ formulation, a model-following control law may be obtained such that perfect model following is achieved asymptotically, as the actuation bandwidth becomes infinite. Let the cost function (19) be modified to include control rate instead of control deflection, or let

$$J_3 = \int_0^\infty [(\dot{e}+Ee)^TQ(\dot{e}+Ee)+\rho\dot{u}^TR\dot{u}]\,dt \tag{23}$$

with the system dynamics represented by

$$\begin{bmatrix} \dot{x}_v \\ \dot{u} \\ \dot{x}_m \\ \dot{\delta} \end{bmatrix} = \begin{bmatrix} A_v & B_v & 0 & 0 \\ 0 & 0 & 0 & 0 \\ 0 & 0 & A_m & B_m \\ 0 & 0 & 0 & A_P \end{bmatrix} \begin{bmatrix} x_v \\ u \\ x_m \\ \delta \end{bmatrix} + \begin{bmatrix} 0 \\ I \\ 0 \\ 0 \end{bmatrix} u$$

Then

$$\dot{e} + Ee = [(C_vA_v + GC_v) \quad C_vB_v \quad -(C_mA_m + GC_m) \quad -C_mB_m] \times \begin{bmatrix} x_v \\ u \\ x_m \\ \delta \end{bmatrix}$$

The resulting control law is of the form

$$\dot{u} = -K_u u - Kx_v - K_m x_m - K_\delta \delta$$

or

$$u(s) = (sI + K_u)^{-1} u_c(s) \tag{24}$$

with

$$u_c = -Kx_v - K_m x_m - K_\delta \delta$$

The finite asymptotic properties of this system will be the same as those described previously. That is, as ρ goes to zero in Eq. (23), the resulting control law would be the same as the one obtained from the formulation with Eq. (19) and with $R \to 0$. Therefore, the previous LQ formulation will lead asymptotically to a closed-loop system with finite poles defined by the transmission zeros in Eq. (20).

The poles introduced due to $(sI + K_u)^{-1}$ in Eq. (24), which can be interpreted as actuator dynamics, will approach infinity as $\rho \to 0$. Harvey and Stein[15] have shown ways in which the cost function weightings Q and R can be chosen to reflect desired directions for these poles. This method has been used by Anderson and Schmidt[16] to tradeoff model-following fidelity (closeness to perfect model following) and required actuator bandwidth.

For subsequent analysis, the first-order approximate actuator dynamics that result from such a model-following synthesis can be replaced by their actual (perhaps higher order) dynamics, and the synthesized control law will be well approximated as long as the crossfeeds [off-diagonal elements in $(sI + K_u)^{-1}$] are retained in $C_a(sI - A_a)^{-1}B_a$ in Eq. (22).

Example 2

As another example, consider the linearized model of the forward swept-wing aircraft described by Gilbert et al.[17] The longitudinal-axis model possesses a short-period, predominantly rigid-body mode coupled with an aeroelastic wing bending mode. The state-space descriptions of the aircraft and the model to be followed are listed in Table 3. The inputs available for control of the aircraft are a full span flaperon deflection δ_f and a canard deflection δ_c. The aircraft input vector is then defined as $u = [\delta_f \text{ (deg)}, \delta_c \text{ (deg)}]^T$. The aircraft responses of interest are pitch rate q and angle of attack α, and so the output vector is $y = [q \text{ (deg/s)}, \alpha \text{ (deg)}]^T$. The airframe is statically unstable, with poles at $+1.36$, -2.27, and $-2.66 \pm j68.95$ (rad/s). The airframe model is also nonminimum phase, with transmission zeros at $+0.53 \pm j61.95$ (rad/s).

The desired model dynamics are also listed in Table 3. Note that the state dimensions of the two models differ. The input to the model dynamics is longitudinal stick force δ (lb) and the output of the model is the desired pitch rate q_m and angle of attack α_m so that the desired response is $y_m = [q_m \text{ (deg/s)}, \alpha_m \text{ (deg)}]^T$.

First-order, homogeneous error dynamics were chosen for this example, with $E = 10I_2$ and $e = y - y_m$. The bandwidth of the error dynamics was chosen higher than the natural frequency of the fastest mode of the desired model (2.0 rad/s) so that loop gain crossover will be sufficiently high. The error responses are also decoupled due to the diagonal E, so that an error in one response will not induce an error in the other response.

Because the bare airframe has right-half-plane transmission zeros, the direct state-space model-following control gains, obtained from Eq. (5), are inappropriate. The LQ formulation, defined in Eq. (19), will be utilized instead. The error-dynamic weighting Q was chosen as $Q = I_2$. The control weighting matrix R was chosen as $R = \rho I_2$.

The state-feedback gains that result with a control weighting parameter value of $\rho = 1d - 06$ are listed in Table 4. The closed-loop system poles consist of the desired model poles at $-1.4 \pm j1.43$ (rad/s) and the poles of $A - BK$. As expected,

Table 3 Example 2—aircraft and model dynamics

	Aircraft dynamics			
$A =$	− 7.3600D − 01	1.0000D + 00	1.6000D − 02	− 8.6000D − 04
	3.1800D + 00	− 1.6600D − 01	− 4.2200D − 02	3.5000D − 03
	0.0000D + 00	0.0000D + 00	0.0000D + 00	1.0000D + 00
	− 2.5937D + 03	1.7650D + 01	− 4.7637D + 03	− 5.3400D + 00
$B =$	− 0.0015	− 0.0019		
	− 0.0140	0.0430		
	0.0000	0.0000		
	− 4.3800	0.2200		
$C =$	0.0000	57.3000	0.0000	0.1500
	57.3000	0.0000	0.0000	0.0000
	Model dynamics			
$A_m =$	0.0000	1.0000		
	− 4.0000	− 2.8000		
$B_m =$	0.0000			
	0.0370			
$C_m =$	40.1100	57.3000		
	57.3000	0.0000		

Table 4 Model-following control gains

$K =$	− 3.4902D + 03	− 5.4833D + 02	1.9755D + 02	− 4.2836D − 01
	− 2.1224D + 03	− 9.3692D + 01	− 1.7166D + 02	1.1129D − 01
$K_m =$	3.8792D + 03	5.1478D + 02		
	2.1981D + 03	1.1953D + 02		
$K_\delta =$	0.6176			
	− 0.4882			

Table 5 Model-following control gains with first-order actuators

$K =$	− 3.2978D + 03	− 2.6713D + 03	3.4716D + 03	7.8908D + 00
	1.2490D + 03	5.2608D + 03	− 1.1729D + 03	− 2.5229D + 01
$K_m =$	4.9642D + 03	2.0221D + 03		
	− 7.0078D + 02	− 3.8794D + 03		
$K_u =$	11.0100	− 10.3929		
	− 10.3929	30.8740		
$K_\delta =$	1.0380D + 01			
	− 2.4479D + 01			

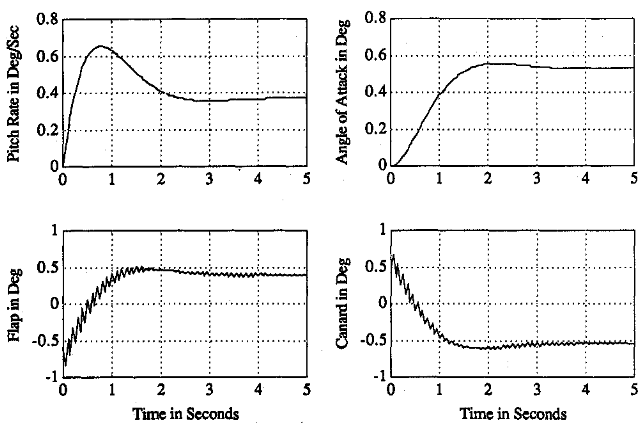

Fig. 4 Time responses—example 2.

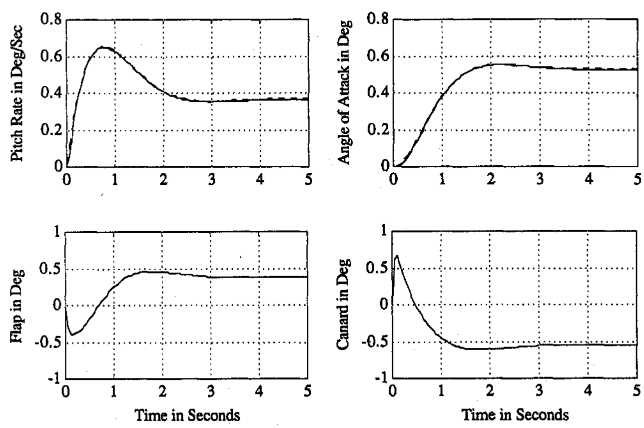

Fig. 5 Time responses with actuators—example 2.

the poles of $A - BK$ are the desired error dynamic poles, which are -10.0, -10.0 (rad/s), and the stable mirror image of the bare airframe transmission zeros, or $-0.53 \pm j61.95$ (rad/s).

Time responses of the closed-loop system are shown in Figs. 4 for a stick step input of unit magnitude. The responses of the model and augmented vehicle are plotted, but the curves are indistinguishable, indicating near perfect model-following fidelity. The control surface responses for this stick step input are also shown. One can see from both the flaperon and canard surface responses that very high surface rates are required in order to achieve the model-following accuracy indicated.

To reduce the rates to something more reasonable, a second set of control gains was synthesized by weighting control surface rates in the model-following cost function defined by Eq. (23). The control-surface-rate weighting matrix R was chosen as $R = \rho I_2$ and the error-dynamic weighting was again chosen as $Q = I_2$. The parameter ρ was then reduced until the diagonal elements of the control surface feedback gains in K_u reached values consistent with production actuator bandwidths.

The state-feedback control gains that result with a control rate weighting parameter of $\rho = 0.01$ are listed in Table 5. The diagonal elements of K_u, reflecting the required actuator time constants, are 11.0 and 30.9 (rad/s) for the full-span flaps and canard, respectively. The poles of the augmented aircraft with these actuator dynamics are at $-2.55 \pm j2.26$, -10.00, -23.85, and $-4.09 \pm j68.46$ (rad/s). The poles at -10.00 and -23.85 result from the presence of the first-order actuators and will asymptotically approach infinity. The other poles are those that will approach the desired error-dynamic poles and the stable mirror image of the finite transmission zeros as ρ is reduced. Recall the value of ρ is limited by the requirement for realistic actuation bandwidths. Consequently, the poles at $-2.55 \pm j2.26$ and $-4.09 \pm j68.46$ do not exactly equal the selected error-dynamic poles and the transmission zeros of the aircraft, respectively.

Time responses of this closed-loop system are shown in Figs. 5, again for a unit stick step. The pitch-rate and angle-of-attack responses are shown as solid lines. The dashed lines are the comparable model responses. One can see that the model-following fidelity has degraded slightly from the responses without actuator dynamics shown in Figs. 4. However, much more realistic control responses are obtained with no ringing in the control surface deflections.

In summary, this example has demonstrated that excellent model-following fidelity can be obtained via the LQ formulation with an appropriate choice of the error dynamics. The location of the bare airframe transmission zeros and the requirement for realistic actuation bandwidth in this example dictated an LQ model-following approach.

Conclusions

The significance of the model-following error dynamics has been the main theme of this paper, and this significance was addressed by developing a unifying theoretical framework. In general, the plant dynamics, model dynamics, and error dynamics are all constrained if perfect model following is to be achieved. The relations between these dynamics and the resulting system characteristics were also explored. It was shown that implicit model following as well as integral action in the control law results from special choices of error dynamics. Relationships between the plant, model, and error dynamics and the closed-loop stability and system transmission zeros were also established.

The new LQ formulation of the model-following problem presented herein establishes a direct link between the algebraic and the LQ model-following approaches and directly employs the error dynamics. It was revealed that the identical control law will result from both solution methods, when the system is square, *CB* of full rank, and the plant possesses no right-half-plane transmission zeros. Unlike the algebraic approach, however, the LQ formulation may be used to synthesize a model-following control law for any system and will guarantee a stable solution for a nonminimum phase plant. It also provides a means by which a tradeoff in model-following fidelity and required actuator bandwidth can be achieved.

Acknowledgments

This research was supported in part by a contract from the McDonnell Aircraft Company, SOW WS-AD-2038. E. H. Anderson served as the technical manager. The work was also supported by NASA Dryden/Ames Research Center under Grant NAG4-1. Don Berry was the technical monitor.

References

[1]Rynaski, E. G., Reynolds, P. A., and Shed, W. H., "Design of Linear Flight Control Systems Using Optimal Control Theory," ASD-TDR-63-376, Wright-Patterson AFB, OH, April 1964.

[2]Tyler, J. S., "The Characteristics of Model-Following Systems as Synthesized by Optimal Control," *IEEE Transactions on Automatic Control,* Vol. AC-9, No. 4, 1964, pp. 485–498.

[3]Chan, Y. T., "Perfect Model-Following with a Real Model," *Proceedings of the Joint Automatic Control Conference,* Columbus, OH, June 1973, pp. 287–293.

[4]Davison, E. J., "The Feedforward Control of Linear Multivariable Time-Invariant Systems," *Automatica,* Vol. 9, 1973, pp. 561–573.

[5]Kawahata, N., "Model-Following System with Assignable Error Dynamics and Its Application to Aircraft," *Journal of Guidance and Control,* Vol. 3, No. 6, 1980, pp. 508–516.

[6]Buethe, S., and Lebacqz, J. V., "Optimal State-Rate Feedback Explicit Model-Following," AIAA Paper 84-1857, Aug. 1984.

[7]Erzberger, H., "Analysis and Design of Model-Following Control Systems by State Space Techniques," *Proceedings of the Joint Automatic Control Conference,* Univ. of Michigan, Ann Arbor, MI, June 1968, pp. 572–581.

[8]Morse, A. S., "Structure and Design of Linear Model Following Systems," *IEEE Transactions on Automatic Control,* Vol. AC-18, No. 4, 1973, pp. 346–354.

[9]Kudva, P., and Gourishankar, V., "On the Stability Problem of Multivariable Model-Following Systems," *International Journal of Control,* Vol. 24, No. 6, 1976, pp. 801–805.

[10]Davison, E. J., and Wang, S. H., "Properties and Calculation of Transmission Zeros of Linear Multivariable Systems," *Automatica,* Vol. 10, 1974, pp. 643–658.

[11]Asseo, S. J., "Application of Optimal Control to Perfect Model Following," *Journal of Aircraft,* Vol. 7, No. 4, 1970, pp. 308–313.

[12]Roskam, J., *Airplane Flight Dynamics and Automatic Flight Controls,* Roskam Aviation and Engineering Corp., Ottawa, KS, 1982.

[13]Kwakernaak, H., and Sivan, R., *Linear Optimal Control Systems,* Wiley, New York, 1972.

[14]Lehtomaki, N. A., Sandell, N. R., and Athans, M., "Robustness Results in Linear-Quadratic Gaussian Based Multivariable Control Designs," *IEEE Transactions on Automatic Control,* Vol. AC-26, No. 1, 1981, pp. 75–92.

[15]Harvey, C. A., and Stein, G., "Quadratic Weights for Asymptotic Regulator Properties," *IEEE Transactions on Automatic Control,* Vol. AC-23, No. 3, 1978, pp. 378–387.

[16]Anderson, M. R., and Schmidt, D. K., "Formulating an Integrated Flight Control Law Synthesis Strategy," AIAA Paper 86-2711, Oct. 1986.

[17]Gilbert, M. G., Schmidt, D. K., and Weisshaar, T. A., "Quadratic Synthesis of Integrated Active Controls for an Aeroelastic Forward-Swept-Wing Aircraft," *Journal of Guidance, Control, and Dynamics,* Vol. 7, No. 2, 1984, pp. 190–196.